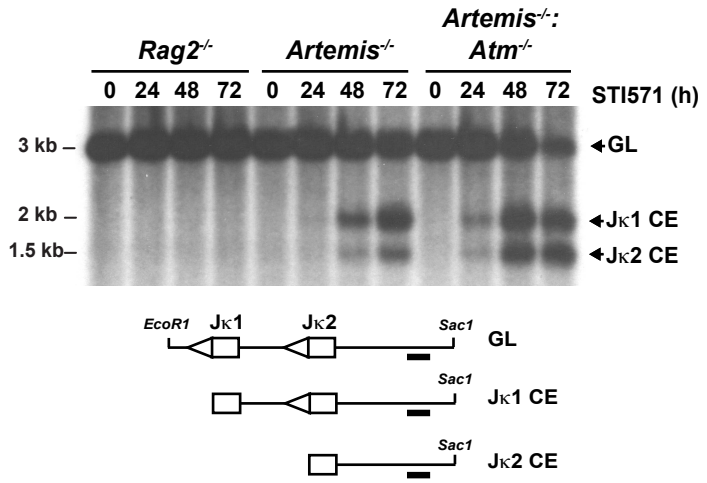


**Supplementary Figure 1. Cleavage at the IgLκ locus in abl pre-B cells.** Southern blot analysis of Rag DSBs (coding ends, CEs) generated at the Jκ gene segments in the IgLκ locus in cells treated with STI571 for the indicated number of hours. Bands generated by the germline (GL) IgLκ locus and Jκ1 and Jκ2 CEs are indicated. The schematic of the products shows the relative positions of the restriction sites (*EcoRI* and *SacI*) and probe (filled rectangle) used for analysis.

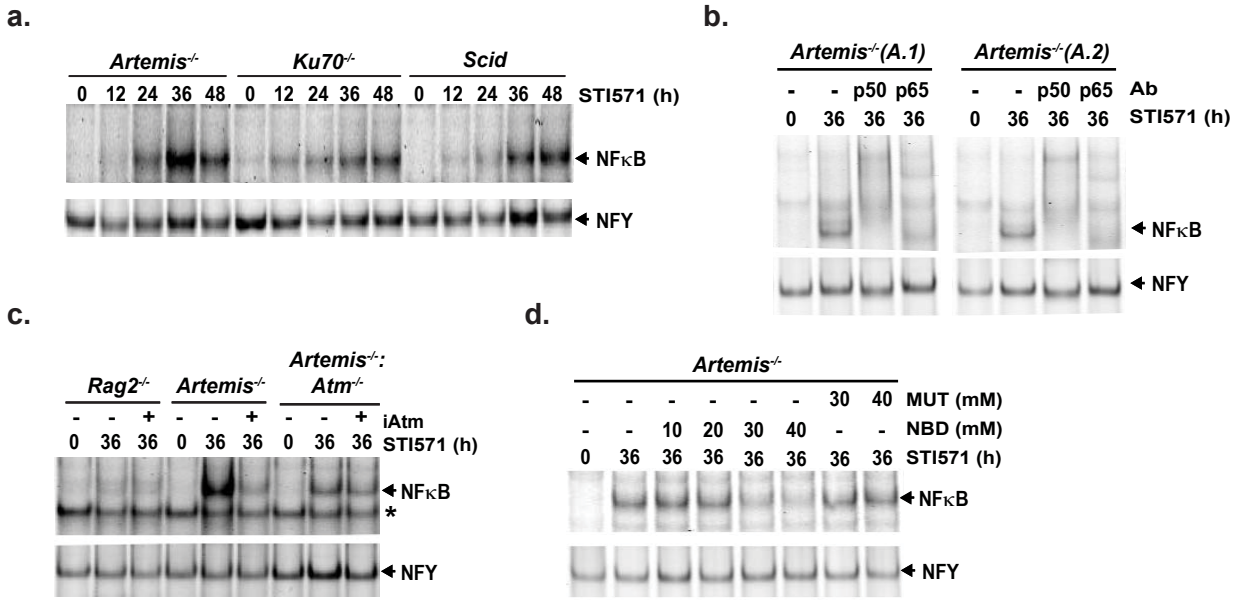


**Supplementary Figure 2. Atm dependent activation of the classical NFκB pathway by Rag DSBs** **(a)** NFκB EMSA of nuclear lysates from *Artemis*$^{-/-}$, *Ku70*$^{-/-}$ and *Scid* (DNAPKcs-deficient) abl pre-B cells treated with STI571 for the indicated times. **(b)** NFκB supershift using antibodies to p50 or p65. Analyses of two independent *Artemis*$^{-/-}$ abl pre-B cells are shown. **(c)** NFκB EMSA of cells treated with STI571 in the presence or absence of the Atm inhibitor KU-55933 (iAtm). Asterisk indicates a non-specific band. **(d)** NFκB EMSA of *Artemis*$^{-/-}$ abl pre-B cells treated with STI571 in the presence of increasing concentrations of either a cell-permeable NEMO binding domain peptide (NBD) or a control cell-permeable NBD mutant peptide (MUT). NFY EMSAs are shown as loading controls.

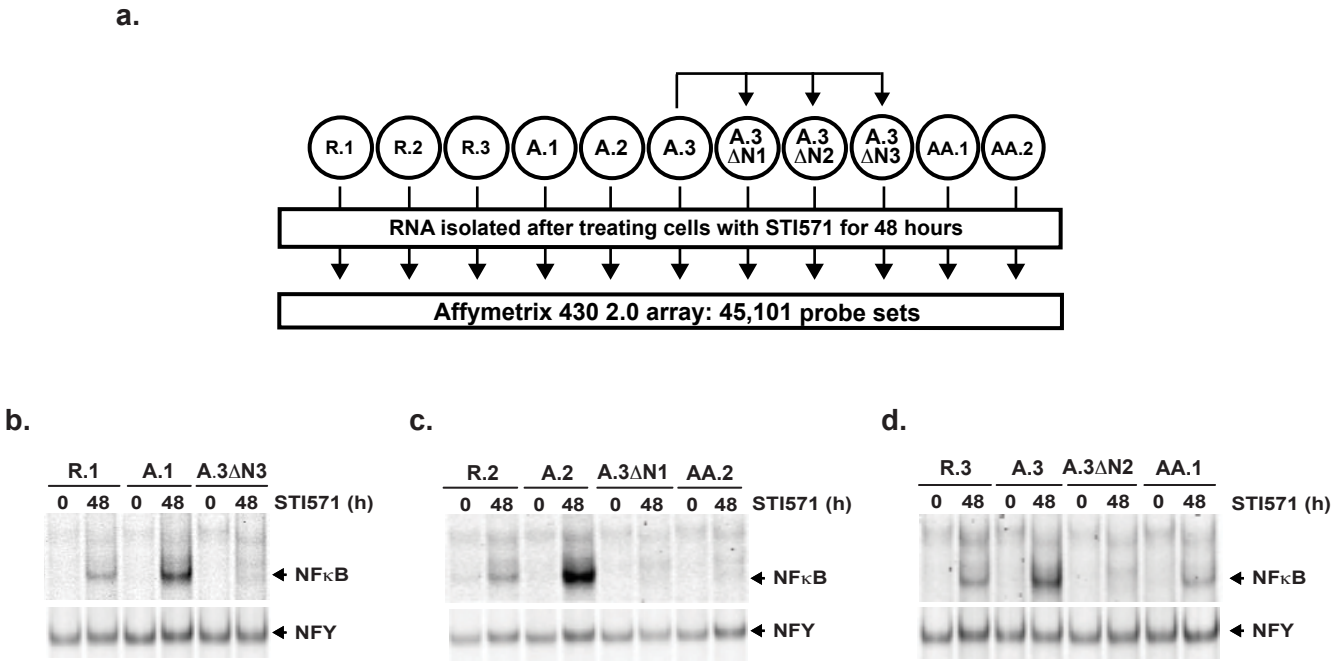


**Supplementary Figure 3. Rag DSB-responsive gene expression profiling (a)** Schematic of the gene expression profiling approach using abl pre-B cells. Shown are three independent *Rag2*$^{-/-}$ cell lines (R.1, R.2 and R.3), three independent *Artemis*$^{-/-}$ cell lines (A.1, A.2 and A.3), two independent *Artemis*$^{-/-}$*:Atm*$^{-/-}$ cell lines (AA.1 and AA.2), and three *Artemis*$^{-/-}$ cell lines that express an IκBα dominant negative, IκBα-ΔN, generated by transfection of the A.3 cell line (A.3ΔN1, A.3ΔN2, A.3ΔN3). **(b-d)** NFκB EMSA of nuclear lysates from abl pre-B cells used for gene expression profiling, treated with STI571 for either 0 or 48 h.

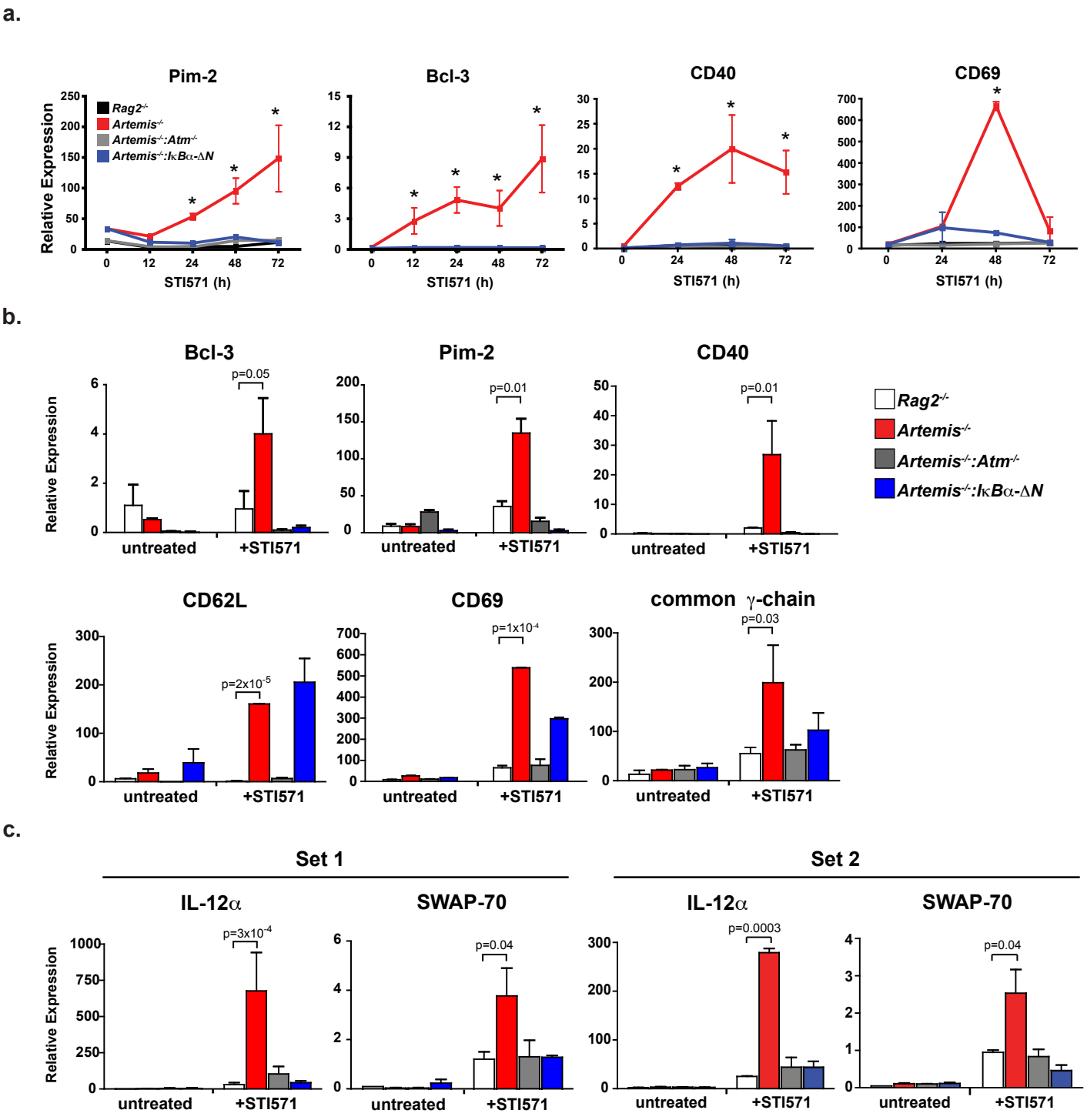


**Supplementary Figure 4. NFκB- and Atm-dependence of Rag DSB-responsive genes.** **(a)** RT-PCR analysis of gene expression in abl pre-B cells treated with STI571 for different periods of time. Abl pre-B cells analyzed were the same as those analyzed in Fig. 1c. Asterisks indicate that the difference between the *Rag2*$^{-/-}$ and *Artemis*$^{-/-}$ cell lines is significant ($p<0.05$). **(b)** The expression of genes analyzed in Fig. 1c was analyzed in additional independent abl pre-B cell lines for each genotype un-treated or treated with STI571 for 48 hours. **(c)** Expression of SWAP-70 and IL-12α in the abl pre-B cells analyzed in Fig. 1c (Set 1) and panel b (Set 2). Genotypes are as indicated in panel b. All values are mean and standard deviation from two experiments. P values were calculated using a one-tailed t-test.

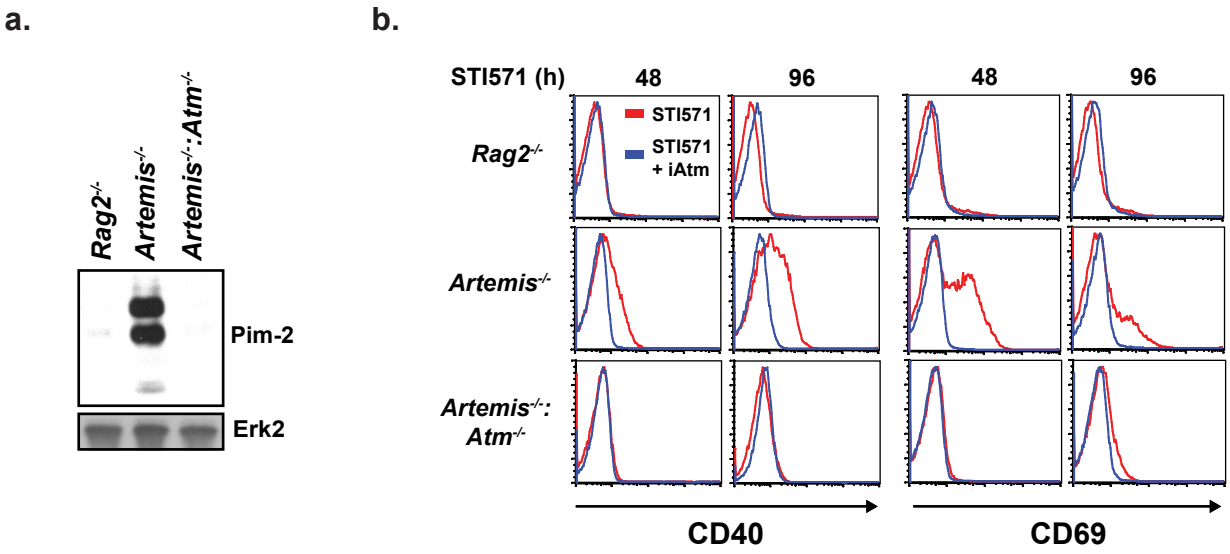


**Supplementary Figure 5. Protein expression in response to Rag DSBs in abl pre-B cells.** **(a)** Western blot analysis of Pim-2 expression in abl pre-B cells treated with STI571 for 48 hours. The three isoforms of Pim-2 are shown. Erk2 is shown as a protein loading control. **(b)** Flow cytometric analysis of CD40 and CD69 protein expression on abl pre-B cells treated with STI571 for 48 or 96 h. Red histogram represents cells treated with STI571 alone; blue histogram represents cells treated with STI571 and KU-55933 (iATM).

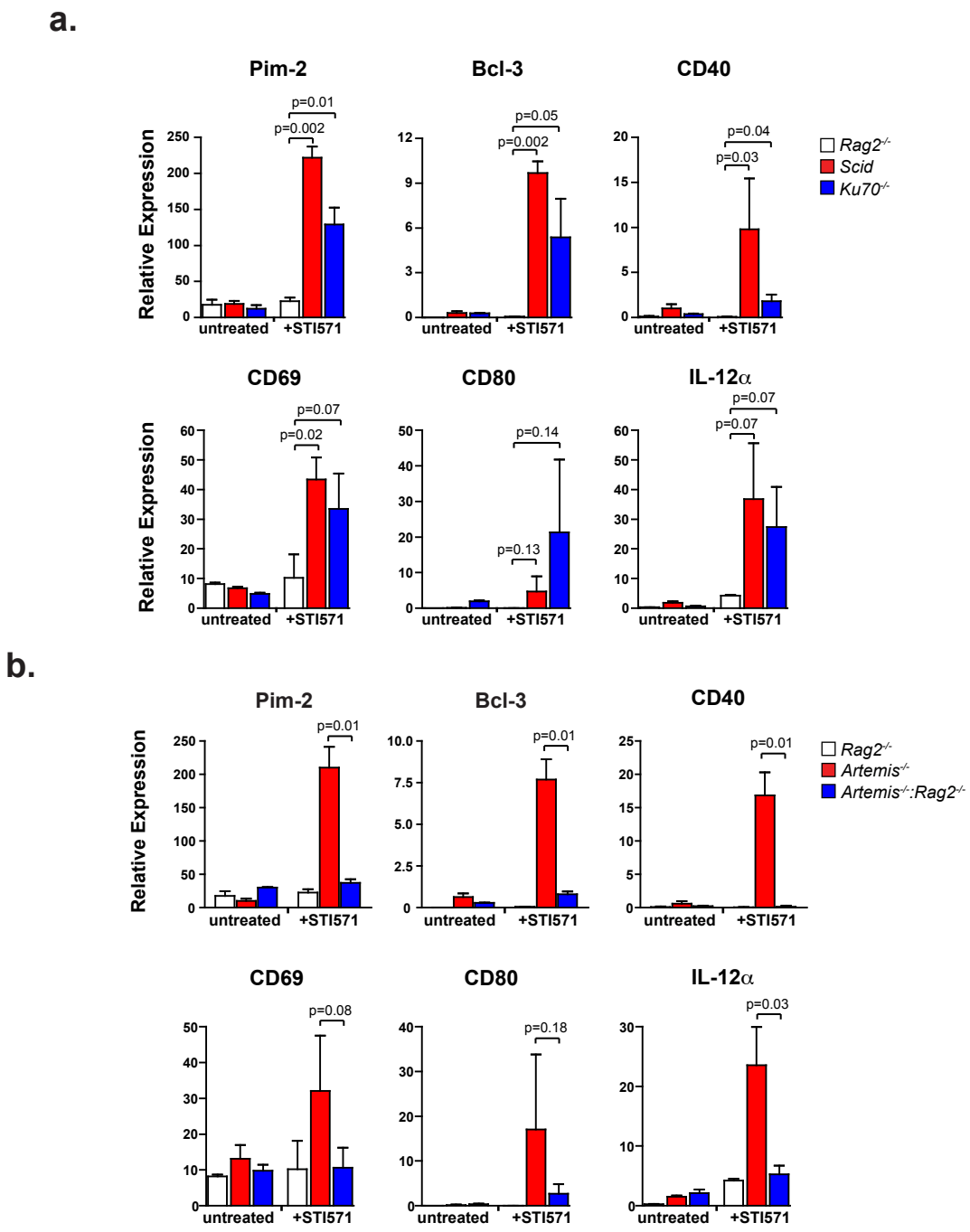


**Supplementary Figure 6. Rag DSB-dependent gene expression changes occur in diverse NHEJ-deficient backgrounds.** RT-PCR analysis of expression of the indicated genes in untreated and STI571-treated (48 h) **(a)** *Rag2*$^{-/-}$, *scid*, and *Ku70*$^{-/-}$ abl pre-B cells or **(b)** *Rag2*$^{-/-}$, *Artemis*$^{-/-}$, and *Artemis*$^{-/-}$*:Rag2*$^{-/-}$ abl pre-B cells. Values are mean and standard deviation from two experiments. P values were calculated using a one-tailed t-test.

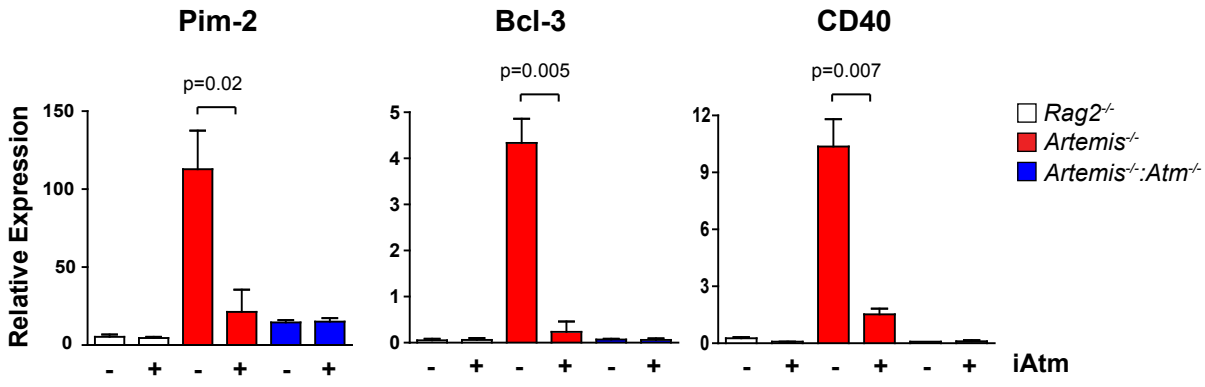


**Supplementary Figure 7. Atm dependence of Rag DSB-responsive gene expression in *Artemis*$^{-/-}$ abl pre-B cells.** RT-PCR analysis of Pim-2, Bcl-3 and CD40 expression in abl pre-B cells treated with STI571 for 24 hours in the presence or absence of the Atm kinase inhibitor KU-55933 (iAtm). Values are mean and standard deviation from two experiments. P values were calculated using a one-tailed t-test.

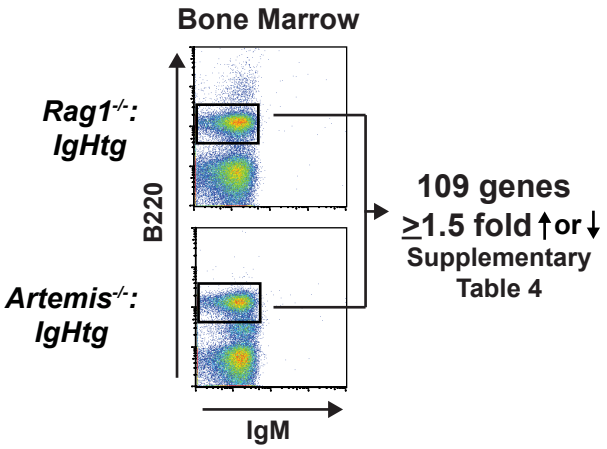


**Supplementary Figure 8. Schematic of gene expression analysis carried out on bone marrow pre-B cells.** Gene expression profiling was carried out on RNA isolated from purified $B220^{+}$:$IgM^{-}$ cells from the bone marrow of *Rag1*$^{-/-}$*:IgHtg* and *Artemis*$^{-/-}$*:IgHtg* mice. The individual genes and expression data are reported in Supplementary Table 4.

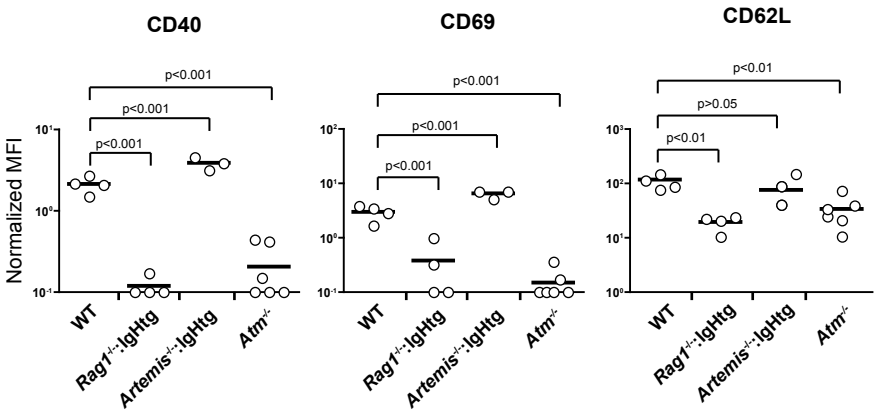


**Supplementary Figure 9. Surface expression of proteins encoded by Rag DSB-responsive genes by developing bone marrow B cells.** Normalized geometric mean fluorescence index (MFI) for CD40, CD69 and CD62L expression on $B220^{+}$:$IgM^{-}$ bone marrow B cells from multiple mice for each genotype. P values were calculated using one-way ANOVA, followed by Bonferroni's Multiple Comparison Test.

**a.**

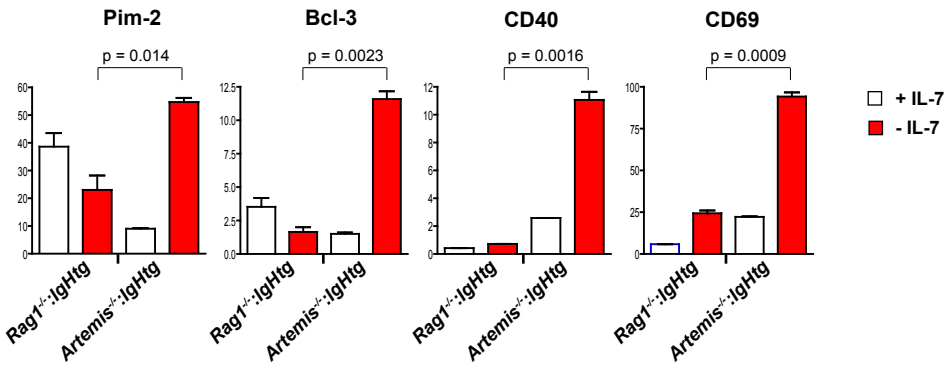


**b.**

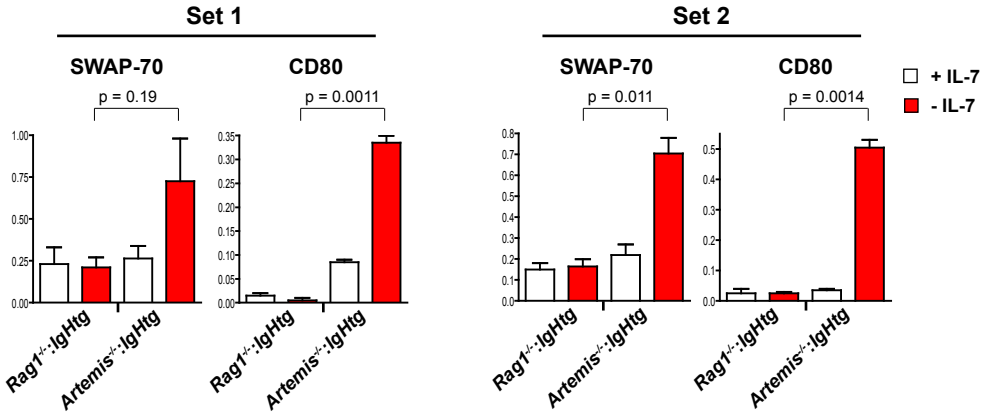


**Supplementary Figure 10. Rag DSB-responsive gene expression in IL-7 dependent bone marrow cultures. (a)** RT-PCR analysis of gene expression in bone marrow cultures derived from different (from those in Fig. 2b) *Rag1$^{-/-}$:IgHtg* and *Artemis$^{-/-}$:IgHtg* mice before (+IL-7, white bars) and 48 hours after (-IL-7, red bars) IL-7 withdrawal. **(b)** RT-PCR analysis of SWAP-70 and CD80 expression in IL-7 cultures analyzed in Fig. 2b (Set 1) and panel a (Set 2). additional genes from the two independent IL-7 dependent bone marrow cultures shown in Figure 2 and in (a). All values are mean and standard deviation from two experiments. P values were calculated using a one-tailed t-test.

**a.**

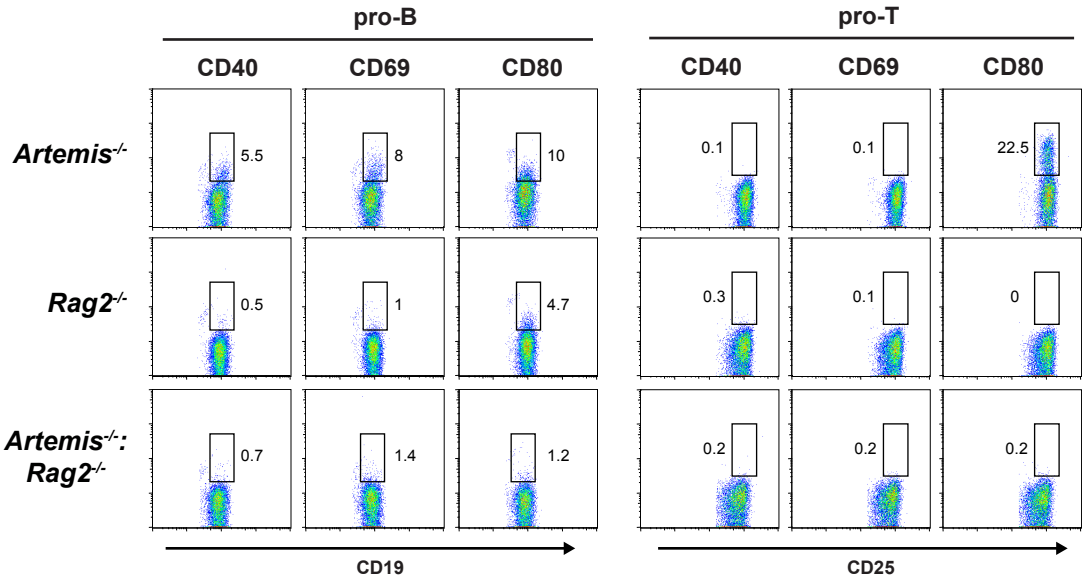


**b.**

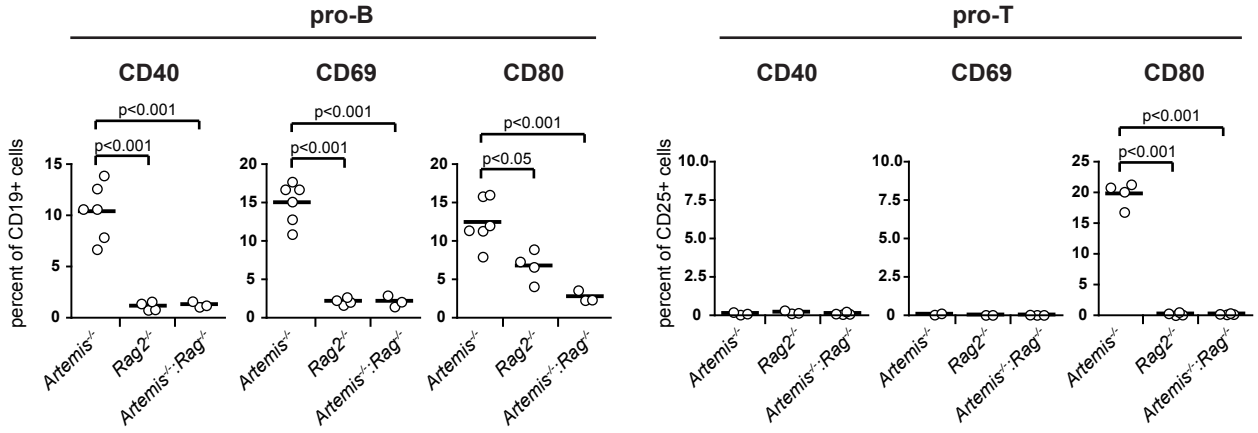


**Supplementary Figure 11. Rag DSB-dependent gene expression in pro-B and pro-T cells.** **(a)** Representative flow cytometric analysis of CD40, CD69 and CD80 expression on pro-B cells (CD19$^+$ bone marrow cells) and pro-T cells (CD25$^+$ thymocytes) from *Rag2*$^{-/-}$, *Artemis*$^{-/-}$ and *Artemis*$^{-/-}$*:Rag2*$^{-/-}$ mice. Percent of cells expressing each gene is indicated. **(b)** Percent of pro-B or pro-T cells expressing the indicated genes in multiple mice. Bar indicates mean percentage of positive cells. P values were calculated using one-way ANOVA, followed by Bonferroni's Multiple Comparison Test.

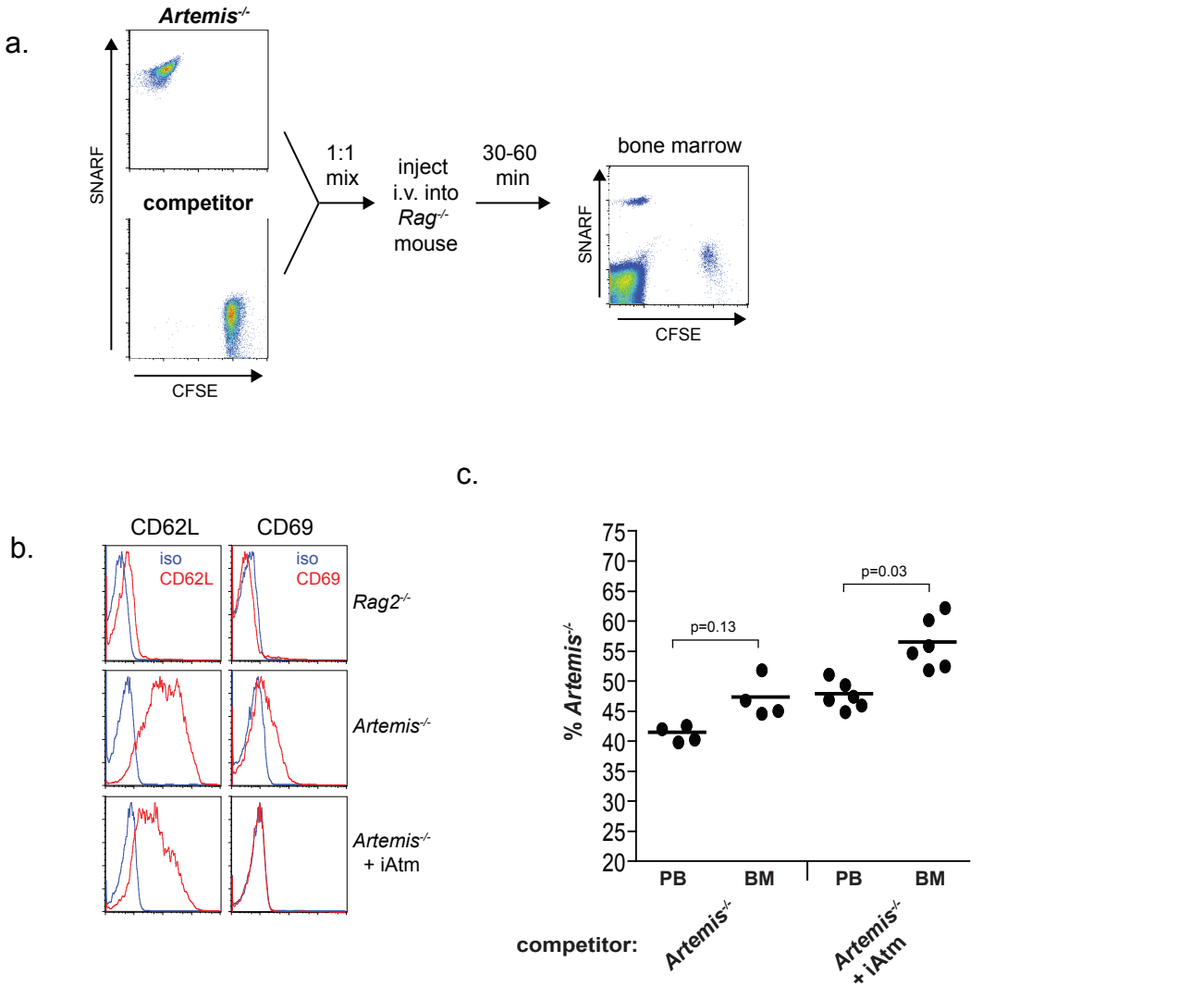


**Supplementary Figure 12. Analysis of competitive abl pre-B cell trafficking.** **(a)** Schematic of co-injection experiment. STI571-treated *Artemis*$^{-/-}$ abl pre-B cells were labeled with the fluorescent dye SNARF and STI571-treated competitor abl pre-B cells were labeled with CFSE. Labeled cells were mixed at a 1:1 ratio and injected into *Rag*$^{-/-}$ mice. Bone marrow and peripheral blood were harvested and analyzed 30-60 minutes later. The competitor cells were Rag-2-/- abl pre-B cells in Fig. 2c and as indicated in panel c. **(b)** Flow cytometry of STI571-treated abl pre-B cells immediately prior to injection. **(c)** Analysis of *Artemis*$^{-/-}$ abl pre-B cell localization in peripheral blood (PB) and bone marrow (BM) of Rag-deficient mice after co-injection at a 1:1 ratio with either competitor *Artemis*$^{-/-}$ abl pre-B cells or competitor *Artemis*$^{-/-}$ abl pre-B cells treated with the KU-55933 Atm inhibitor (iAtm). Shown is the percentage of injected cells in PB and BM that were non-competitor *Artemis*$^{-/-}$ abl pre-B cells. The line indicates the mean of the set of mice analyzed. P values were calculated using a two-tailed Wilcoxon match pairs test.

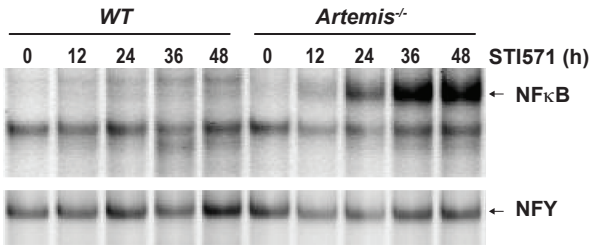


**Supplementary Figure 13. NFκB activation in response to Rag DSBs in wild type and Artemis-deficient cells.** NFκB EMSA of nuclear lysates from wild type (WT) and *Artemis*$^{-/-}$ abl pre-B cells treated with STI571 for the indicated times. NFY EMSA is shown as a control.

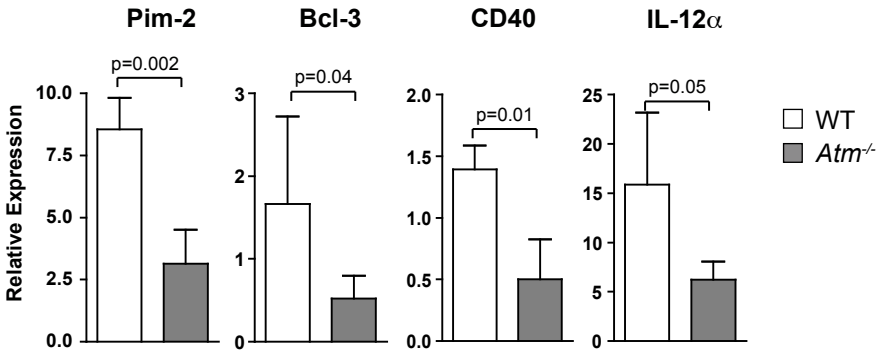


**Supplementary Figure 14. Atm-dependent gene expression in response to transient Rag DSBs in B220$^+$:IgM$^-$ bone marrow B cells.** RT-PCR analysis of expression of the indicated genes in purified WT (white bar) and *Atm*$^{-/-}$ (grey bar) B220$^+$:IgM$^-$ bone marrow B cells. Results are the mean and standard deviation of analyses done on cells from three mice. P values were calculated using a one-tailed t-test.

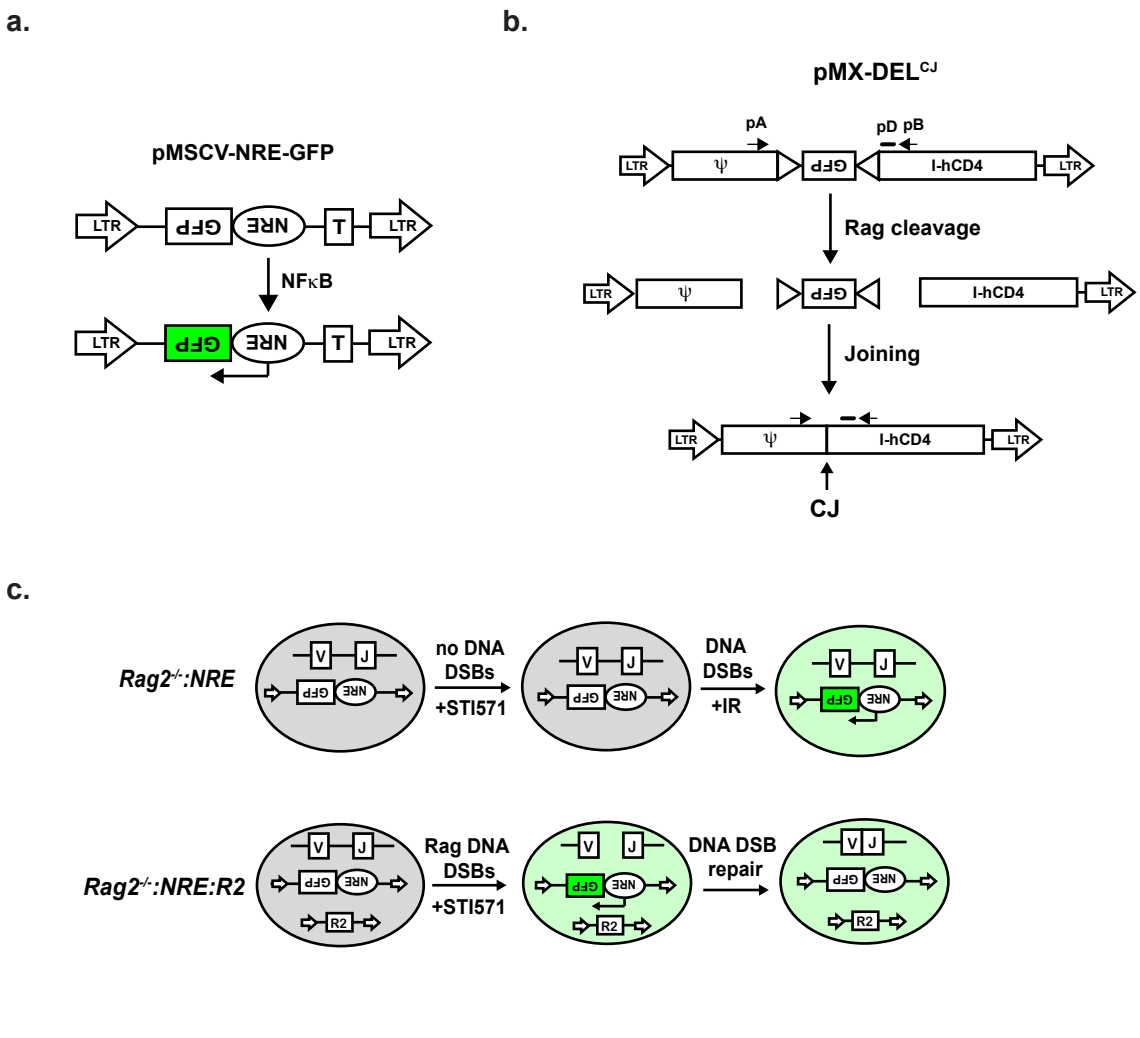


**Supplementary Figure 15. Analysis of NFκB activation in abl pre-B cells.**
**(a)** Schematic of the pMSCV-NRE-GFP retrovirus, showing the Thy1 cDNA (T), the five tandem NFκB responsive elements (NRE), and the GFP cDNA in the anti-sense orientation. **(b)** Schematic of the pMX-DEL$^{CJ}$ retroviral recombination substrate described in reference 14. Shown is the GFP cDNA in the anti-sense orientation flanked by RSs (open triangles). Also shown are the IRES-human CD4 (I-hCD4) cassette, the long terminal repeats (LTRs), and the retroviral packaging sequence (Ψ). The relative position of the pC and pB oligonucleotides (arrows) used for PCR analysis of coding joint (CJ) formation and the pD oligonucleotide (bar) used to probe the PCR products are also shown. **(c)** Schematic of pMSCV-NRE-GFP activation and GFP expression by treated and untreated *Rag2$^{-/-}$:NRE* and *Rag2$^{-/-}$:NRE:R2* cells. Transcription of the NRE-GFP cassette is indicated by the filled arrow from NRE and green shading of the GFP cDNA rectangle. The cessation of GFP transcription, as indicated by the white filled GFP cDNA rectangle, after repair of Rag-mediated DSBs is presumed. The presence of GFP in the cell is indicated by green shading of the cell. Rag DSBs are indicated by the discontinuity between the V and J gene segment, and a coding joint is indicated by the juxtaposition of the V and J gene segment. The retrovirally introduced Rag2 cDNA in *Rag2$^{-/-}$:NRE:R2* cells is shown (R2).

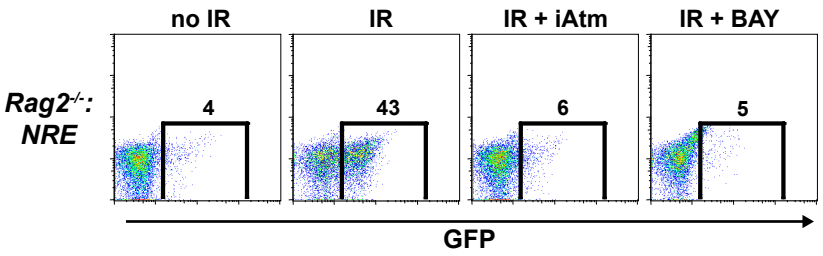


**Supplementary Figure 16. Activation of NFκB in *Rag2*$^{-/-}$*:NRE* cells in response to IR induced DSBs.** *Rag2*$^{-/-}$*:NRE* abl pre-B cells were treated with STI571 for 24 hours, then either not irradiated (no IR) or irradiated with 0.5 Gy (IR) and treated with vehicle alone, the Atm inhibitor KU-55933 (iAtm), or the inhibitor of IκB phosphorylation, BAY 11-7085 (BAY). Cells were analyzed for GFP expression from pMSCV-NRE-GFP by flow cytometry 12 hours post-irradiation.

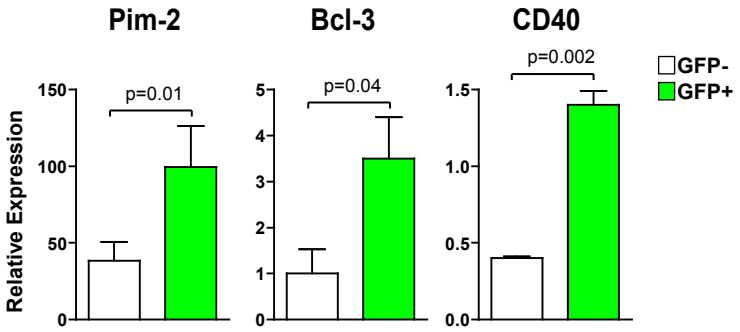


**Supplementary Figure 17. Gene expression in *Rag2*$^{-/-}$*:NRE:R2* cells in response to transient Rag DSBs.** RT-PCR of Pim-2, Bcl-3 and CD40 expression in sorted GFP$^{+}$ and GFP$^{-}$ *Rag2*$^{-/-}$*:NRE:R2* cells following 48 h of treatment with STI571. Results are the mean and standard deviation of two experiments; p values were calculated using a one-tailed t-test.

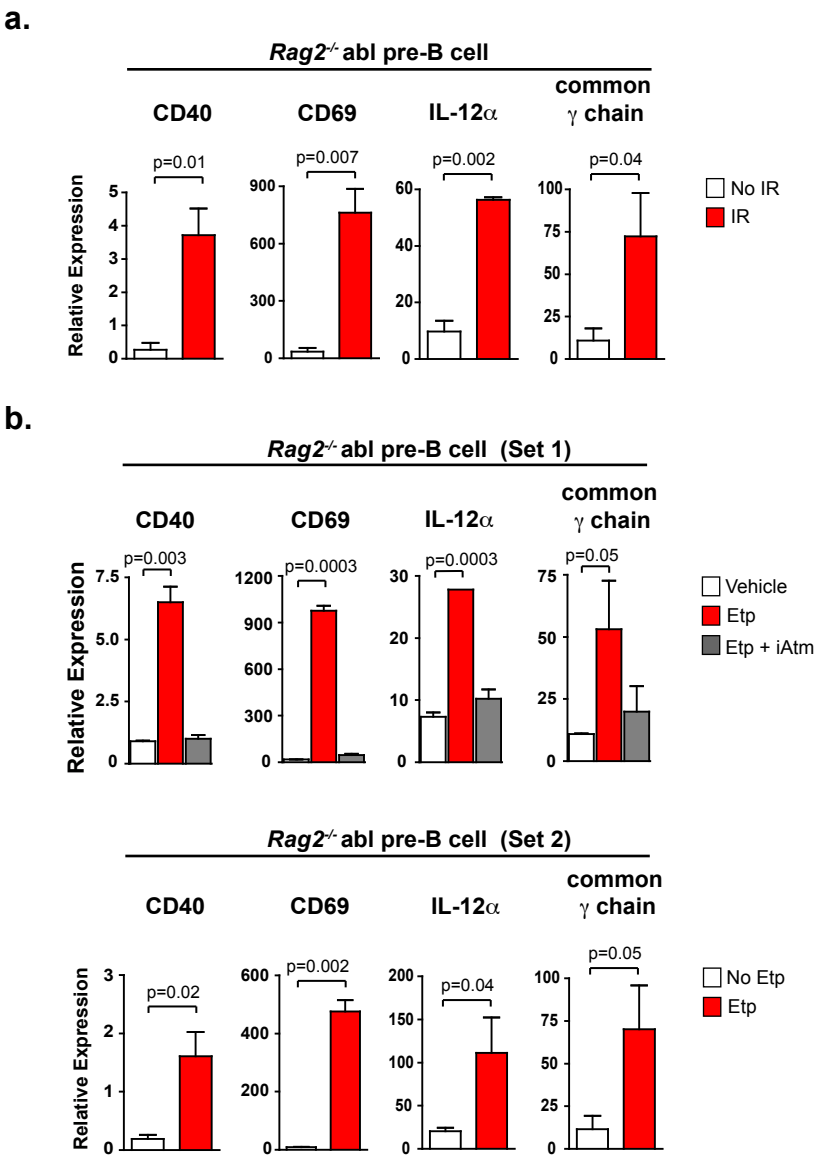


**Supplementary Figure 18. Genotoxic agents induce expression of lymphocyte-specific genes in abl pre-B cells. (a)** An additional (different from Fig. 4a) independent *Rag2*$^{-/-}$ abl pre-B cell line was analyzed by RT-PCR for expression of the indicated genes in response to 4 Gy irradiation. Cells were treated with STI571 for 24 hours prior to irradiation. **(b)** RT-PCR analysis of *Rag2*$^{-/-}$ abl pre-B cell lines for expression of the indicated genes in response to treatment with 5μM etoposide (Etp). The *Rag2*$^{-/-}$ abl pre-B cell lines analyzed here are the same as those analyzed in Fig. 4a (Set 1) and panel a (Set 2). These cells were treated with STI571 for 24 hours prior to etoposide treatment. The set 1 analysis also included etoposide treatment with the Atm inhibitor (iAtm). All values are means and standard deviations from two experiments. P values were calculated using a one-tailed t-test.